Distinct duration and diet dependent lipid profiles and renal complications in GCK-MODY

Yadi Huang[1,#], Yuxin Fan[1,#], Yang Liu[1,#], Xuan Liu[1], Wei Li[1], Ying Yang[1], Ziyue Zhang[1], Shifeng Ma[1], Shuhui Ji[1], Shanshan Chen[1], Hua Shu[1], Wenli Feng[1], Kunlin Wang[1], Qing He[1], Wenjun Qi[2], Yu Fan[1,‡], Xin Li[1,‡], Ming Liu[1,‡]

[1]Department of Endocrinology and Metabolism, Tianjin Medical University General Hospital, Tianjin, 300052, China

[2]NHC Key Laboratory of Hormones and Development, Chu Hsien-I Memorial Hospital and Institute of Endocrinology, Tianjin Medical University, Tianjin, 300134, China

[#]Authors contribute equally to the work.

[‡]To whom correspondence may be addressed. Ming Liu, Department of Endocrinology and Metabolism, Tianjin Medical University General Hospital, #154 Anshan Road, Heping District, Tianjin, 300052, China. Email: mingliu@tmu.edu.cn; Yu Fan, Email: fanyu5@hotmail.com; Xin Li, email: lixin920616@163.com.

Corresponding author:

Ming Liu[1,‡] M.D., Ph.D.

Email: mingliu@tmu.edu.cn

Tel: +86-22-60817182

Address: Department of Endocrinology and Metabolism, Tianjin Medical University General Hospital, 154 Anshan Road, Heping District, Tianjin, China 300052

Distinct duration and diet dependent lipid profiles and renal complications in GCK-MODY

Yadi Huang[1,#], Yuxin Fan[1,#], Yang Liu[1,#], Xuan Liu[1], Wei Li[1], Ying Yang[1], Ziyue Zhang[1], Shifeng Ma[1], Shuhui Ji[1], Shanshan Chen[1], Hua Shu[1], Wenli Feng[1], Kunlin Wang[1], Qing He[1], Wenjun Qi[2], Yu Fan[1,‡], Xin Li[1,‡], Ming Liu[1,‡]

Abstract

Heterozygous inactivating mutations in the glucokinase (GCK) gene cause one of the most common types of maturity-onset diabetes of the young type 2 (MODY2), also named GCK-MODY. Studies suggest that, unlike other types of diabetes, patients with GCK-MODY do not have increased risk of diabetic complications and therefore do not typically require antihyperglycemic therapy. However, long-term outcomes of GCK-MODY on lipid profiles and chronic complications under different dietary scenarios remain unclear. Herein, using a knock-in mouse model expressing a novel MODY causing mutation GCK-Q26L (GCK^{Mut}), we examined age- and diet-related lipid profiles and diabetic complications. We found that, although GCK^{Mut} mice exhibited mild elevated blood glucose, the lipid profiles, body fat composition, and diabetic kidney disease (DKD) were initially improved in high-fat-diet (HFD) fed mice at the age of 28 weeks, supporting potential beneficial effects of GCK^{Mut} on lipid metabolism and kidney health. Unexpectedly however, those protective effects diminished by 40 weeks, and became more severe dyslipidemia and kidney injury associated with renal fibrosis and inflammation at 60-week-old mice fed with normal diet (ND) or HFD. Those findings revealed distinct duration- and

diet-dependent effects of inactivating GCK mutation on lipid profiles and DKD, highlighting previously unrealized long-term chronic complications in GCK-MODY.

Keywords: Glucokinase, GCK-MODY, Lipid profiles, Diabetic kidney disease

1. Introduction

Glucokinase (GCK), a glycolytic enzyme belonging to the hexokinase family, plays a pivotal role in catalyzing the conversion of glucose into glucose-6-phosphate, a primary step in glucose metabolism within pancreatic β-cells and hepatocytes [1-3]. Heterozygous inactivating mutations in the GCK gene cause maturity-onset diabetes of the young type 2 (MODY2, also named GCK-MODY), which is one of the most common types of monogenic diabetes [4-6]. Patients with GCK-MODY typically present mild to moderate non-progressive elevated fasting blood glucose (FBG) without significant abnormalities or even improvement of lipid metabolism [7, 8]. More importantly, current evidence indicates that individuals with GCK-MODY are not associated with increased risks of chronic diabetic complications compared to the other types of diabetes [9]. Therefore, current consensuses suggest that such patients may not necessitate pharmacological interventions [10, 11].

However, due to the limited number of patients diagnosed with GCK-MODY, there is a paucity of prospective interventional or observational studies examining the long-term outcomes of GCK-MODY under different dietary conditions. Additionally, given the potential impact of persistent hyperglycemia on ocular, vascular, neurological and renal diseases [12-15], it is important to investigate long-term effects of inactivating GCK mutations on lipid metabolism and functional and structural alterations in microvascular complications associated with prolonged hyperglycemia.

Recently, we have established a knock-in mouse line expressing a novel GCK mutation (GCK-Q26L, GCK^{Mut}) identified in two members of a family with early onset diabetes, and

92 demonstrated that this mutation indeed impaired insulin secretion causing mild elevated FBG
93 and impaired glucose tolerance that mirrors the phenotypes of patients with GCK-MODY
94 (https://doi.org/10.1101/2024.08.13.24311668). In this study, using this knock-in mouse model,
95 we examined age- and diet-related lipid profiles and diabetic complications in the GCK-MODY.
96 We found that GCK mutant indeed presented beneficial effects on lipid metabolism, body fat
97 composition, and renal injury in high-fat-diet (HFD) fed GCK^{Mut} mice at the age of 28 weeks.
98 However, those protective effects diminished with time, and more severe dyslipidemia and
99 kidney injury associated with renal fibrosis and inflammation were observed in GCK^{Mut} mice fed
100 with HFD at the age of 60 weeks. Those findings revealed distinct duration- and diet-dependent
101 effects of inactivating GCK mutation on body composition, lipid profiles, and diabetic kidney
102 disease (DKD), highlighting previously unrealized long-term metabolic abnormalities and
103 chronic diabetes complications in GCK-MODY. This is poised to offer valuable insights for the
104 prevention and treatment of individuals diagnosed with GCK-MODY aiming to improve long-
105 term reduction of chronic complications. Given the fact that decreased expression and function
106 of GCK are also seen in type 2 diabetes [16], this study may also have clinical implications in the
107 management of type 2 diabetes (T2D).
108

109 **2. Methods and Materials**

110 **2.1 Animal models**

111 Male WT mice were purchased from SPF Biotechnology, while a global GCK-Q26L (GCK^{Mut})
112 knock-in mouse line was established as described in our previous study. Both GCK^{Mut} mice and
113 WT mice were housed in pathogen-free conditions within the the Laboratory Animal Center of
114 Tianjin Medical University Chu Hsien-I Memorial Hospital. WT and GCK^{Mut} male mice were

115 randomly assigned to four groups and subjected to either a normal diet (ND; comprising 20%
116 protein, 4% fat, 5% fiber, SCXK(LU) 2018-0003) or a high-fat diet (HFD; comprising 20%
117 protein, 60% fat, 20% carbohydrates, D12492, Research Diets) from four weeks of age until they
118 reached 28, 40, and 60 weeks of age. Throughout this period, monitoring of body weight and
119 blood glucose levels was conducted every 4 weeks. All mice utilized in the study were
120 maintained on a C57BL/6J background and housed in a 12 h light/dark cycle in a temperature
121 (22–25 °C) and humidity (55 ± 5%) control room.
122

123 **2.2 Biochemical measurements**

124 Blood glucose levels were assessed using an automated glucometer (Roche, ACCU-CHEK,
125 Germany). Mice were placed in metabolic cages to collect 24-hour urine samples. Various
126 parameters including serum total cholesterol (TC), triglycerides (TG), low-density lipoprotein
127 cholesterol (LDL-c), high-density lipoprotein cholesterol (HDL-c), serum creatinine, 24-hour
128 urinary albumin excretion (UAE), and urinary creatinine were determined by kits provided from
129 Nanjing Jiancheng Institute of Bioengineering (Nanjing, China).
130

131 **2.3 Intraperitoneal glucose tolerance test and insulin tolerance test**

132 The intraperitoneal glucose tolerance test (IPGTT) involved the intraperitoneal administration of
133 1 g/kg body weight of glucose in mice following a 6-hour fasting period. The area under the
134 curve (AUC) was determined using the trapezoidal rule. Simultaneously, blood samples collected
135 at each time point were utilized to measure blood glucose and serum insulin levels employing an
136 insulin ELISA assay kit (EZassay, China), following the manufacturer's instructions. For the
137 intraperitoneal insulin tolerance test (IPITT), mice that fasted for 4 hours received an

138 intraperitoneal injection of 0.75 U/kg body weight of insulin. Tail vein glucose levels were
139 monitored at 0, 15, 30, 60 and 120 minutes post-injection. All experiments mentioned above
140 were conducted using age- and sex-matched cohorts.
141
142 **2.4 Body composition measurements**
143 Fat mass of was measured using a Bruker Minispec mq7.5 (Brucker).
144
145 **2.5 Histologic evaluation and transmission electron microscopy anslysis**
146 Following anesthesia, mice were euthanized subsequently the kidneys were harvested， which
147 were fixed in 4% paraformaldehyde, then paraffin-embedded and were cut into 5-μm-thick
148 sections. Subsequently, these sections were stained, and after sealing with neutral balsam, images
149 were captured using AxioImagerM2 (Carl Zeiss, Oberkochen, Germany). The extent of kidney
150 injury within each group was assessed utilizing Image-ProPlus 6.0 software. The sections
151 underwent staining procedures involving hematoxylin and eosin (H&E), Periodic acid-Schiff's
152 (PAS), and Masson's trichrome. For semi-quantitative analysis, twenty stained glomeruli per
153 section were randomly chosen (5 mice per group) for analyses. For transmission electron
154 microscopy (TEM), fresh isolated kidney tissues were sliced into small pieces and then fixed in
155 2.5% glutaraldehyde for a duration of 12 hours. Subsequently, the tissues underwent treatment
156 with 1% osmium tetroxide. Ultrathin sections were obtained utilizing an ultramicrotome
157 (LeicaEMUC7, Germany), followed by a dehydration process using gradient alcohol,
158 permeabilization with acetone, and final embedding in epoxy. The obtained ultrathin sections,
159 measuring between 70-90 nm, were stained with uranyl acetate and lead citrate. These sections
160 were examined using a transmission electron microscope (TEM) (HT7700, Japan).

161

162 **2.6 RNA Extraction, cDNA Synthesis, and Quantitative real-time PCR (qRT-PCR)**

163 Total RNA was extracted and purified from renal tissues using TRIzol reagent (Invitrogen, USA).
164 Subsequently, cDNA was synthesized utilizing the PrimeScriptTM RT kit with gDNAEraser
165 (Takara, Japan), following the manufacturer's instructions. qRT-PCR assays were conducted in a
166 20 μL reaction volume employing TB Green Premix Ex Taq^{TM} (Tli RNaseH Plus) (Takara,
167 Japan). GAPDH served as the internal control. The primers utilized in this study were designed
168 and chemically synthesized by ZTSINGKE Biological Technology (Beijing, China) Co. Ltd.
169 Details of the primer sequences were provided in **Supplemental Table S1**.

170

171 **2.7 Protein Extraction and Western Blot Analysis**

172 Renal tissues were lysed using RIPA lysis buffer for protein extraction. Protein samples were
173 then loaded onto SDS-PAGE, electrophoretically separated, and subsequently transferred to
174 nitrocellulose membranes. These membranes were blocked using 5% skimmed milk followed by
175 blotted with indicated antibodies, and visualized by enhanced chemiluminescence (CLiNX,
176 Shanghai, China). The following antibodies were utilized in this study: anti-E-Cadherin (A3044;
177 ABclonal), anti-Vimentin (A11423; ABclonal), anti-α-SMA (A7248; ABclonal), anti-IL-1β
178 (A16288; ABclonal), anti-TNF-α (A11534; ABclonal), and anti-β-actin (KM9001T, Sungene).

179

180 **2.8 Transcriptome analysis**

181 Renal transcriptome analysis was conducted by BGI Group, encompassing RNA extraction,
182 library preparation, and sequencing. Data processing adhered to the standard BGI mRNA
183 analysis pipeline. Statistical analysis was executed utilizing the Deseq2 software package

184 (v1.28.1). Differentially expressed genes (DEGs) were identified using a threshold of log2 (fold
185 change) absolute value ⩾ 1 and false discovery rate ⩽ 0.05. For further insights, Gene Ontology
186 (GO) analysis was carried out using cluster/profiler (v3.16.1). Pathway visualization was
187 accomplished using GraphPad Prism 8.
188
189 **2.9 Statistics**
190 Statistical analyses were conducted utilizing GraphPad Prism 8 software. The data are presented
191 as mean ± standard deviation. Analysis involved unpaired Student's t-tests, with statistical
192 significance set at the traditional critical value of $P < 0.05$. Each experiment was independently
193 repeated at least three times.
194
195 **3. Results**
196 **3.1 GCK^{Mut} impairs insulin secretion, leading to elevated FBG, but improves lipid profiles**
197 **in early normal diet (ND) mice**
198 We have monitored body weight (BW) and FBG of ND fed mice every 4 weeks until 60 weeks
199 of age, and found that GCK^{Mut} caused non-progressively mild elevated FBG without affecting
200 BW (**Fig. 1A-B**). To evaluate the effect of GCK^{Mut} on insulin secretion and glucose tolerance,
201 we performed intraperitoneal glucose tolerance tests (IPGTT) at the ages of 28, 40, and 60 weeks,
202 respectively. We found that GCK^{Mut} resulted in impaired glucose tolerance associated (**Fig. 1C-E,**
203 **Fig. S1A-C**) with decreased basal and glucose stimulated insulin secretion (**Fig. 1F-H, Fig.**
204 **S1D-F**). However, GCK^{Mut} did not appeared to affect insulin sensitivity during intraperitoneal
205 insulin tolerance tests (IPITT) (**Fig. 1I-K, Fig. S1G-I**). Next, we examined body composition
206 and lipid profiles of GCK^{Mut} mice, and found that although GCK^{Mut} did not change the body fat

207 composition, the weight of perirenal white adipose tissue (pWAT), and the weight of gonadal
208 white adipose tissue (gWAT) (**Fig. 1L-N**), it indeed decreased levels of serum triglyceride (TG)
209 and low-density protein cholesterol (LDL-c) in 28-week-old mice. However, those beneficial
210 effects on lipid metabolism diminished at 40 and 60 weeks of age (**Fig. 1O-R**). Those data
211 demonstrate that decreased activity of GCK causes mild non-progressive hyperglycemia with
212 improved lipid profiles at young age and this improvement waned over time.
213

214 **3.2 Exacerbation of proteinuria and renal pathological changes in 60-week-old GCK^{Mut}**
215 **mice fed with ND**

216 Hyperglycemia is associated with microvascular complications in patients with T2D [17, 18].
217 Given the elevated blood glucose in patients with GCK-MODY, it is important to determine the
218 long-term effects of GCK-MODY on chronic diabetic complications. We therefore measured
219 kidney weight (KW) and BW and found no significant difference in the KW/BW ratio between
220 GCK^{Mut} and control mice at 28, 40, and 60 weeks of age (**Fig. 2A**). Additionally, in comparison
221 to WT mice, GCK^{Mut} mice displayed no differences in the levels of 24-hour urinary albumin
222 excretion (UAE), urinary albumin-to-creatinine ratio (UACR), and serum creatinine at 28 and 40
223 weeks of age. However, UAE, UACR, and serum creatinine were notably increased at 60 weeks
224 of age in GCK^{mut} mice (**Fig. 2B-D**). Histological analyses demonstrated relatively normal
225 glomerular and tubular morphology and structure in GCK^{Mut} mice at 28 and 40 weeks of age.
226 PAS and Masson staining indicated marginal differences in thylakoid dilation and renal fibrosis
227 between GCK^{Mut} and control mice at 28 and 40 weeks, which exacerbated notably at 60 weeks of
228 age (**Fig. 2E-G and K-L**). Subsequently, we utilized transmission electron microscopy to
229 examine glomerular structure at 28, 40, and 60 weeks of age in both groups of mice. The

230 observations indicated a trend of increased thickness of glomerular basement membrane (GBM)
231 at 28 and 40 weeks of age, and a significant thickening of GBM was evident at 60 weeks of age
232 in GCK^{Mut} mice (**Fig. 2H-J and M**).
233

234 **3.3 Renal fibrosis- and inflammation-associated genes exhibit high expression in aging**
235 **GCK^{Mut} mice fed with ND**

236 To investigate pathways involved in long-term renal changes in GCK^{mut} mice, we performed
237 transcriptome analysis using kidneys from littermate controls and GCK^{Mut} mice. Gene Ontology
238 (GO) analysis of the two groups of mice at 60-week-old age revealed that the 940 differentially
239 expressed genes (DEGs, with $|Log2|$ fold change ≥ 1 and false discovery rate ≤ 0.05), which
240 were primarily enriched in collagen fibril organization, cell-matrix adhesion, and inflammatory
241 response (**Fig. 3A**), consistent with previous reports indicating that excessive accumulation of
242 extracellular mesenchymal tissue and pro-inflammatory responses contribute to the progression
243 of DKD [19-21]. We further analyzed the DEGs involved in biological progression of DKD, and
244 found that Vim (Vimentins, encoding intermediate filaments), Acta2 (α-SMA, encoding alpha-
245 smooth muscle actin), Col1a1 (COL1A1, encoding type I collagen) and Tnf exhibited significant
246 up-regulation in GCK^{Mut} mice at 60 weeks of age (**Fig. 3B**). The changes of the these genes were
247 further confirmed by quantitative real-time PCR (qRT-PCR) excepted Colla1 that did not show a
248 statistic difference between two groups. The gene Cdh1 (cadherin 1, encoding E-cadherin),
249 which maintains stable cellular connections and cellular architecture integrity [22], was
250 significantly downregulated (**Fig. 3C**). Furthermore, Western blot analysis verified that the
251 protein levels of Vim, α-SMA, TNF-α and IL-1β were indeed significantly elevated in the
252 kidneys of 60-week-old GCK^{Mut} mice, whereas no significant changes in proteins levels and

253 mRNA levels were observed in 28- and 40-week-old mice (**Fig. 3D-G, Fig. S2**). These results
254 suggest that upregulation of the genes associated with renal fibrotic and inflammatory responses
255 may be attributed to long-term kidney injury in the old GCK^{mut} mice.
256

257 **3.4 The lipid profile of 28-week-old GCK^{Mut} mice fed with HFD improved, but worsened at**
258 **60 weeks**

259 A recent study has revealed that partial inactivation of GCK can yield beneficial effects on
260 hepatic lipid metabolism and inflammation [23]. These effects have been postulated as a
261 potential rationale behind the favorable lipid profile and reduced cardiovascular risk observed in
262 patients with GCK-MODY [24, 25]. Our data indicated that although improved circulating lipid
263 profiles were indeed validated at early time in GCK^{Mut} mutant mice, those improvements
264 diminished over the time in mice fed with ND (**Fig. 1O-R**). We therefore asked what effects of
265 additional metabolic stress inactivation of GCK on glucolipid metabolism and renal injury. We
266 randomly grouped 4-week-old littermate mutant and control mice for the HFD regimen while
267 maintaining the same experimental protocols as those used for mice fed with ND. Our findings
268 revealed a transient small but statistic decrease in body weight in 28-week-old GCK^{Mut} mice fed
269 with HFD. However, this divergence disappeared in the mice fed with HFD till 40- and 60-week-
270 old (**Fig. 4A**). Additionally, elevated fasting and postprandial blood glucose (**Fig. 4B-E, Fig.**
271 **S3A-C**), decreased circulating insulin (**Figs. 4F-H, Fig. S3D-F**), and insulin sensitivity (**Figs. 4I-**
272 **K, Fig. S3G-I**) had all similar trends as that we observed in mice fed with ND. These data
273 further demonstrate that although elevated FBG and impaired glucose intolerance persist, these
274 diabetes phenotypes are stable and are not aggravated even under HFD in GCK^{mut} mice.
275

276 Next, we analyzed body composition and revealed a significant reduction in fat mass in HFD fed
277 GCK^{Mut} mice at 28 weeks in comparison to the control group (**Fig. 4L**). Similarly, pWAT and
278 gWAT (**Fig. 4M-N**) as well as serum TC and LDL-c levels displayed noteworthy reductions
279 along with elevated HDL-c in HFD fed GCK^{Mut} mice at 28 weeks (**Fig. 4O-R**). However, at 40
280 to 60 weeks of age, the aforementioned indices were progressively worse, resulting in significant
281 deleterious changes of lipid profiles at the age of 60 weeks (**Fig. 4S-V**). These data suggest that
282 long-term exposure of hyperglycemia and HFD may override the potential beneficial effects of
283 GCK^{Mut} on lipid metabolism and body composition, manifesting more severe metabolism
284 disorders.
285

286 **3.5 GCK^{Mut} attenuates HFD induced renal injury at 28 weeks of age, but aggravates renal**
287 **injury at 60 weeks of age**

288 Previous study has indicated that ectopic lipid accumulation in the kidneys contributes to kidney
289 injury [26-28]. Analogous to alterations in lipid profiles, quantitative analysis of lipids extracted
290 from kidneys exhibited significantly reduced TC and TG levels along with decreased kidney
291 weight in GCK^{Mut} mice fed with HFD at the age of 28 weeks. However, with extended exposure
292 to the hyperglycemia and HFD, TC and TG contents in the kidneys of GCK^{Mut} mice gradually
293 increased in comparison to WT mice over time (**Fig. 5A-C, Fig. S4A-B**). To further evaluate
294 renal damage, we also examined 24-hour UAE, UACR, and serum creatinine levels in both
295 groups of mice. The findings revealed reduced UAE, UACR, and serum creatinine levels in
296 GCK^{Mut} mice fed with HFD at the age of 28 weeks, but increased alterations in 60-week-old
297 HFD fed GCK^{Mut} mice (**Fig. 5D-F, Fig. S4C-E**). Notably, histological staining indicated
298 significantly reduced renal mesangial matrix and collagen fiber deposition in GCK^{Mut} mice

299 compared to WT mice fed with HFD at the age of 28 weeks, but these indicators gradually
300 increased at 40 and 60 weeks (**Fig. 5G-I and M-N**). Furthermore, TEM analysis demonstrated a
301 significantly smaller degree of GBM thickness in GCK^{Mut} mice at 28 weeks compared to control
302 mice. However, this thickness significantly increased at 60 weeks (**Fig. 5J-L and O**). These
303 findings indicate that proteinuria progression and pathological damage induced by a HFD were
304 mitigated in GCK^{Mut} mice fed with HFD at early age, whereas long-term (60 weeks) HFD and
305 hyperglycemia worsened renal damage at 60 weeks in GCK^{mut} mice. Altogether, those findings
306 highlight distinct diet and duration dependent effects of GCK inactivating mutation on lipid
307 profiles and the kidney.
308

309 **3.6 GCK^{mut} attenuates the expression of genes associated with renal fibrosis and**
310 **inflammation in 28-week-old HFD fed mice, whereas reversal effects GCK^{mut} on the**
311 **changes of above genes are observed after long-term HFD exposure**

312 To investigate the mechanism of attenuated renal injury in GCK^{Mut} induced by HFD, we
313 conducted transcriptome analyses of renal samples from GCK^{Mut} mice fed with HFD at the age
314 of 28 weeks. GO enrichment analysis revealed that 462 DEGs were predominantly involved in
315 fatty acid metabolic process, extracellular matrix organization, immune system process, cell-
316 matrix adhesion, collagen fibril organization and inflammatory response (**Fig. 6A).** Further
317 analysis of genes enriched in GO highlighted that fibrosis-related genes such as Col1a1 and Vim,
318 and inflammatory cytokines like Tnf were significantly down-regulated. Additionally, genes
319 associated with lipid catabolic process, such as Ppara and Lpl, displayed significant up-
320 regulation (**Fig. 6B).** Subsequently, qRT-PCR confirmed that mRNA levels of Vim, Tnf and
321 Acta2 were significantly reduced and Cdh1, Ppara, whereas Lpl were significantly elevated in

322 the kidneys of GCK^{Mut} mice compared with WT mice (**Fig. 6C**). Western blot also showed that
323 the expression of E-Cadherin was increased, whereas the expression of Vim , α-SMA and TNF-α
324 were decreased in GCK^{Mut} mice fed with HFD at the age of 28 weeks. Importantly, transcriptome
325 analyses confirmed by qRT-PCR and western blotting showed that that the genes linked to renal
326 fibrosis and inflammatory of the above gene expression were reversed in GCK^{mut} mice fed with
327 HFD at the age of 60 weeks (**Fig. 6D-G, Fig. S5**).
328

329 **4. Discussion**

330 GCK-MODY is one of most common types of monogenic diabetes [29]. Patients with GCK-
331 MODY usually exhibit mild and asymptomatic fasting hyperglycemia, persisting from birth with
332 minimal progression over time [4-6]. Generally, the mild elevated blood glucose in GCK-MODY
333 does not require treatment with antidiabetic medications, except during pregnancy [30-32]. One
334 primary rationale for this lies in the markedly low incidence of microvascular and macrovascular
335 complications, nearly akin to those observed in healthy individuals [33, 34]. Previous studies
336 have revealed that patients with GCK-MODY showcase normal metabolic profiles, including
337 relatively lower serum TG with higher HDL-c levels, which may contribute to fewer
338 complications in these patients [35, 36]. However, given the fact that uncontrolled prolonged
339 hyperglycemia is strongly associated with diabetes complications and the lack of perspective
340 studies focusing on patients with GCK-MODY in different dietary settings, the long-term effects
341 of GCK inactivating mutations on chronic complications remain to be further determined.
342

343 In this study, using a newly established mouse model carrying a novel MODY causing GCK
344 mutation, we delved into the impact of the GCK mutant on lipid profiles and diabetic

complications from youth to old age, paying particular attention to a commonly overlooked factors: the combination of mild hyperglycemia and a high-fat diet. We founded a reduction of abnormal lipid profiles and mitigated renal injuries in 28-week-old GCK^{Mut} mice fed with HFD. However, over an extended duration, a tendency towards exacerbated abnormalities in lipid metabolism and heightened renal damage was observed (**Figs. 4-6**). These data revealed surprisingly distinct duration and diet dependent effects of GCK^{Mut} and uncover previously unrecognized pathological significance of prolonged reduction of GCK activity in lipid metabolism and kidney injuries in patients with GCK-MODY. These data may be more informative as controlled experimental variables can minimize complex clinical factors including genetic diversity and use of different medications. These observations warrant further studies in humans.

One of clinical features of patients with GCK-MODY is optimal lipid profile characterizing as significantly lower levels of serum LDL-c and TG along with a higher level of HDL-c compared with nondiabetic control and patients with T2D [24, 36]. A recent study reveals an increased recruitment of adipose triglyceride lipase and choline/ethanolamine phosphotransferase 1 onto the surface of HDLs, resulting in enhanced production of plasmalogen phosphatidylcholines that may confer vascular protection against chronic exposure to hyperglycemia [35]. In this study, we found that although there were decreased levels of serum LDL-c and TG, there were no differences in serum HDL-c between control and GCK^{mut} fed with ND (**Fig. 1**). However, under a metabolic stress (fed with HFD), GCK^{mut} exhibits more beneficial effects not only on levels of HDL-c (**Fig. 4**), but also on renal lipid deposition and injuries (**Fig. 5**) at the age of 28 weeks. These observations suggest that beneficial effects GCK^{mut} on lipid metabolism may override the

368 negative impacts of hyperglycemia on the renal damage at the early stages of diabetes. However,
369 as prolonged hyperglycemia further extends especially under the HFD conditions, these
370 beneficial lipid metabolisms were gradually reversed along with increased proteinuria and renal
371 injuries (**Figs. 2-3 and 5-6**). It remains to be determined whether these paradoxical duration and
372 diet dependent effects of GCK^{Mut} were solely due to extra long-term exposure of hyperglycemia
373 that directly disallows the protective effects of GCK^{Mut} on kidneys, or further prolonged
374 hyperglycemia rejects beneficial effects of GCK^{Mut} on lipid metabolism, resulting more severe
375 abnormal lipid profiles that may in turn damage kidney.
376
377 Recent studies have underscored the pivotal role of inflammation in the pathogenesis of DKD,
378 indicating its significance in triggering metabolic, biochemical, and hemodynamic disturbances
379 in diabetes [37, 38]. DKD, recognized as a chronic, low-grade inflammatory disease, represents a
380 primary feature associated with T2D and its microvascular complications [39-41]. Renal
381 inflammation manifests through immune cell infiltration, cytokine and chemokine release, and
382 activation of inflammatory signaling pathways [42]. Our investigation aligns with these findings,
383 demonstrating that 60-week-old GCK^{Mut} mice, both on a ND or HFD, exhibited more severe
384 renal inflammatory infiltration compared to controls (**Figs. 3 and 6**). Conversely, the observed
385 reduction in renal proteinuria and pathological changes in 28-week-old GCK^{Mut} mice fed with
386 HFD may be associated with diminished inflammatory infiltration. The characteristic
387 pathological hallmark linked with DKD involves the accumulation of extracellular matrix (ECM)
388 components in the glomeruli, often leading to renal angio-glomerulosclerosis and functional
389 decline [19-22]. Our study suggests that GCK^{Mut} may mitigate renal fibrosis by curbing ECM
390 accumulation and expansion of the thylakoid matrix in the early stages of diabetic nephropathy,

391 thereby substantially preserving renal function in diabetic mice. Additionally, previous research
392 has indicated that kidneys of mice on a HFD exhibited notable glomerular and tubular injury,
393 inclusive of substantial defects in the glomerular filtration barrier and heightened tubular cell
394 apoptosis [43, 44]. These effects were possibly linked to increased TC and TG content, alongside
395 activation of the adipogenic pathway in the kidneys [45, 46]. Correspondingly, our observations
396 reinforce these findings, indicating that this protective effect on the kidney wanes or even
397 exacerbates renal injury as the lipid profile deteriorates with prolonged high-fat feeding in
398 GCK^{Mut} mice.
399

400 **5. Conclusions**

401 In summary, our study presents novel evidence emphasizing the pivotal role of GCK in
402 glucolipid metabolism and the progression of diabetic complications. MODY causing GCK
403 mutant benefits lipid metabolism, decreasing renal lipid deposition, inflammatory infiltration,
404 and fibrosis progression in the early stages, thus retarding disease advancement. However, GCK
405 mutant appeared to be associated with exacerbated abnormalities of lipid metabolism and renal
406 injury in later stages. These distinct duration-dependent effects of GCK mutant raise the question
407 regarding current consensus for the management of patients with GCK-MODY.
408

409 **Declarations of interest**

410 The authors declare that no conflicts of interest exist and have no financial interests associated
411 with the present study.
412

413 **Data availability**

414 The authors are willing to make the raw data generated in their study available to other
415 investigators upon reasonable request.
416
417 **Funding**
418 The work was supported by the National Key R&D Program (2022YFE0131400 and
419 2019YFA0802502), and also by the National Natural Science Foundation of China
420 (82220108014, 82100865, and 82301951). We acknowledge the support of Tianjin Key Medical
421 Discipline (Specialty) Construction Project (TJYXZDXK-030A)， Tianjin Municipal Health
422 Commission (TJWJ2021ZD001), Tianjin Municipal Science and Technology Commission
423 (23JCQNJC00680), Tianjin Medical University General Hospital Clinical Research Program
424 (22ZYYLCZD02)， and Tianjin Medical University Clinical Special Disease Research Center -
425 Neuroendocrine Tumor Clinical Special Disease Research Center.
426
427
428 **Author contributions**
429 YH, YF, YF, XL, XL,WQ and YY conducted experiments and analyzed data; YL, WL, ZZ, SM,
430 SJ, SC, HS, KW and WF conducted experiments; QH discussed project and edited manuscript;
431 ML initiated and oversaw the project, designed the experiments, and wrote the manuscript.
432
433 **References**
434 [1] Matschinsky FM. Glucokinase as glucose sensor and metabolic signal generator in pancreatic
435 beta-cells and hepatocytes. Diabetes. 1990;39(6):647-52.

436 [2] Sternisha SM, and Miller BG. Molecular and cellular regulation of human glucokinase. Arch
437 Biochem Biophys. 2019;663:199-213.
438 [3] Bonnefond A, Unnikrishnan R, Doria A, Vaxillaire M, Kulkarni RN, Mohan V, et al.
439 Monogenic diabetes. Nat Rev Dis Primers. 2023;9(1):12.
440 [4] Pulst K, Arbo T, Kahre T, Peet A, and Tillmann V. MODY2 caused by a novel mutation of
441 GCK gene. J Pediatr Endocrinol Metab. 2012;25(7-8):801-3.
442 [5] Shields BM, Hicks S, Shepherd MH, Colclough K, Hattersley AT, and Ellard S. Maturity-
443 onset diabetes of the young (MODY): how many cases are we missing? Diabetologia.
444 2010;53(12):2504-8.
445 [6] Chakera AJ, Steele AM, Gloyn AL, Shepherd MH, Shields B, Ellard S, et al. Recognition and
446 Management of Individuals With Hyperglycemia Because of a Heterozygous Glucokinase
447 Mutation. Diabetes Care. 2015;38(7):1383-92.
448 [7] Hulín J, Škopková M, Valkovičová T, Mikulajová S, Rosoľanková M, Papcun P, et al.
449 Clinical implications of the glucokinase impaired function - GCK MODY today. Physiol Res.
450 2020;69(6):995-1011.
451 [8] Bishay RH, and Greenfield JR. A review of maturity onset diabetes of the young (MODY)
452 and challenges in the management of glucokinase-MODY. Med J Aust. 2016;205(10):480-5.
453 [9] Steele AM, Shields BM, Wensley KJ, Colclough K, Ellard S, and Hattersley AT. Prevalence
454 of vascular complications among patients with glucokinase mutations and prolonged, mild
455 hyperglycemia. Jama. 2014;311(3):279-86.
456 [10] Stride A, Shields B, Gill-Carey O, Chakera AJ, Colclough K, Ellard S, et al. Cross-sectional
457 and longitudinal studies suggest pharmacological treatment used in patients with glucokinase
458 mutations does not alter glycaemia. Diabetologia. 2014;57(1):54-6.

459 [11] Carmody D, Naylor RN, Bell CD, Berry S, Montgomery JT, Tadie EC, et al. GCK-MODY
460 in the US National Monogenic Diabetes Registry: frequently misdiagnosed and unnecessarily
461 treated. Acta Diabetol. 2016;53(5):703-8.
462 [12] Au SC, Tang SM, Rong SS, Chen LJ, and Yam JC. Association between hyperglycemia and
463 retinopathy of prematurity: a systemic review and meta-analysis. Sci Rep. 2015;5:9091.
464 [13] Nieves-Cintrón M, Flores-Tamez VA, Le T, Baudel MM, and Navedo MF. Cellular and
465 molecular effects of hyperglycemia on ion channels in vascular smooth muscle. Cell Mol Life
466 Sci. 2021;78(1):31-61.
467 [14] Tomlinson DR, and Gardiner NJ. Glucose neurotoxicity. Nat Rev Neurosci. 2008;9(1):36-45.
468 [15] Alicic RZ, Rooney MT, and Tuttle KR. Diabetic Kidney Disease: Challenges, Progress, and
469 Possibilities. Clin J Am Soc Nephrol. 2017;12(12):2032-45.
470 [16] Liu J, Fu H, Kang F, Ning G, Ni Q, Wang W, et al. β-Cell glucokinase expression was
471 increased in type 2 diabetes subjects with better glycemic control. J Diabetes. 2023;15(5):409-18.
472 [17] Beckman JA, and Creager MA. Vascular Complications of Diabetes. Circ Res.
473 2016;118(11):1771-85.
474 [18] Stumvoll M, Goldstein BJ, and van Haeften TW. Type 2 diabetes: principles of pathogenesis
475 and therapy. Lancet. 2005;365(9467):1333-46.
476 [19] Xue M, Sun H, Xu R, Wang Y, Guo J, Li X, et al. GADD45B Promotes Glucose-Induced
477 Renal Tubular Epithelial-Mesenchymal Transition and Apoptosis via the p38 MAPK and JNK
478 Signaling Pathways. Front Physiol. 2020;11:1074.
479 [20] Pan Y, Wang Y, Cai L, Cai Y, Hu J, Yu C, et al. Inhibition of high glucose-induced
480 inflammatory response and macrophage infiltration by a novel curcumin derivative prevents
481 renal injury in diabetic rats. Br J Pharmacol. 2012;166(3):1169-82.

482 [21] Wang S, Li Y, Fan J, Zhang X, Luan J, Bian Q, et al. Interleukin-22 ameliorated renal injury
483 and fibrosis in diabetic nephropathy through inhibition of NLRP3 inflammasome activation. Cell
484 Death Dis. 2017;8(7):e2937.
485 [22] Chang YP, Sun B, Han Z, Han F, Hu SL, Li XY, et al. Saxagliptin Attenuates Albuminuria
486 by Inhibiting Podocyte Epithelial- to-Mesenchymal Transition via SDF-1α in Diabetic
487 Nephropathy. Front Pharmacol. 2017;8:780.
488 [23] Xie Z, Xie T, Liu J, Zhang Q, and Xiao X. Glucokinase Inactivation Ameliorates Lipid
489 Accumulation and Exerts Favorable Effects on Lipid Metabolism in Hepatocytes. Int J Mol Sci.
490 2023;24(5).
491 [24] Ping F, Fu J, and Xiao X. Distinguishing the lipid profile of GCK-MODY patients and its
492 correlation with hsCRP levels. Front Endocrinol (Lausanne). 2022;13:1024431.
493 [25] Fendler W, Rizzo M, Borowiec M, Malachowska B, Antosik K, Szadkowska A, et al. Less
494 but better: cardioprotective lipid profile of patients with GCK-MODY despite lower HDL
495 cholesterol level. Acta Diabetol. 2014;51(4):625-32.
496 [26] D'Agati VD, Chagnac A, de Vries AP, Levi M, Porrini E, Herman-Edelstein M, et al.
497 Obesity-related glomerulopathy: clinical and pathologic characteristics and pathogenesis. Nat
498 Rev Nephrol. 2016;12(8):453-71.
499 [27] Xiong W, Xiong Z, Song A, Lei C, Ye C, and Zhang C. Relieving lipid accumulation
500 through UCP1 suppresses the progression of acute kidney injury by promoting the
501 AMPK/ULK1/autophagy pathway. Theranostics. 2021;11(10):4637-54.
502 [28] Chen J, Li T, Vladmir C, Yuan Y, and Sun Z. Renal lipid accumulation induced by high-fat
503 diet regulates glucose homeostasis via sodium-glucose cotransporter 2. Diabetes Res Clin Pract.
504 2021;179:109027.

505 [29] Anık A, Çatlı G, Abacı A, and Böber E. Maturity-onset diabetes of the young (MODY): an
506 update. J Pediatr Endocrinol Metab. 2015;28(3-4):251-63.
507 [30] Timsit J, Ciangura C, Dubois-Laforgue D, Saint-Martin C, and Bellanne-Chantelot C.
508 Pregnancy in Women With Monogenic Diabetes due to Pathogenic Variants of the Glucokinase
509 Gene: Lessons and Challenges. Front Endocrinol (Lausanne). 2021;12:802423.
510 [31] Urakami T. Maturity-onset diabetes of the young (MODY): current perspectives on
511 diagnosis and treatment. Diabetes Metab Syndr Obes. 2019;12:1047-56.
512 [32] Tosur M, and Philipson LH. Precision diabetes: Lessons learned from maturity-onset
513 diabetes of the young (MODY). J Diabetes Investig. 2022;13(9):1465-71.
514 [33] Hattersley AT, Greeley SAW, Polak M, Rubio-Cabezas O, Njølstad PR, Mlynarski W, et al.
515 ISPAD Clinical Practice Consensus Guidelines 2018: The diagnosis and management of
516 monogenic diabetes in children and adolescents. Pediatr Diabetes. 2018;19 Suppl 27:47-63.
517 [34] Gloyn AL. Glucokinase (GCK) mutations in hyper- and hypoglycemia: maturity-onset
518 diabetes of the young, permanent neonatal diabetes, and hyperinsulinemia of infancy. Hum
519 Mutat. 2003;22(5):353-62.
520 [35] Wang X, Lam SM, Cao M, Wang T, Wang Z, Yu M, et al. Localized increases in CEPT1 and
521 ATGL elevate plasmalogen phosphatidylcholines in HDLs contributing to atheroprotective lipid
522 profiles in hyperglycemic GCK-MODY. Redox Biol. 2021;40:101855.
523 [36] Spégel P, Ekholm E, Tuomi T, Groop L, Mulder H, and Filipsson K. Metabolite profiling
524 reveals normal metabolic control in carriers of mutations in the glucokinase gene (MODY2).
525 Diabetes. 2013;62(2):653-61.
526 [37] Pérez-Morales RE, Del Pino MD, Valdivielso JM, Ortiz A, Mora-Fernández C, and
527 Navarro-González JF. Inflammation in Diabetic Kidney Disease. Nephron. 2019;143(1):12-6.

528 [38] Rayego-Mateos S, Rodrigues-Diez RR, Fernandez-Fernandez B, Mora-Fernández C,
529 Marchant V, Donate-Correa J, et al. Targeting inflammation to treat diabetic kidney disease: the
530 road to 2030. Kidney Int. 2023;103(2):282-96.
531 [39] Bonner R, Albajrami O, Hudspeth J, and Upadhyay A. Diabetic Kidney Disease. Prim Care.
532 2020;47(4):645-59.
533 [40] Jung CY, and Yoo TH. Pathophysiologic Mechanisms and Potential Biomarkers in Diabetic
534 Kidney Disease. Diabetes Metab J. 2022;46(2):181-97.
535 [41] Lin YC, Chang YH, Yang SY, Wu KD, and Chu TS. Update of pathophysiology and
536 management of diabetic kidney disease. J Formos Med Assoc. 2018;117(8):662-75.
537 [42] Winiarska A, Knysak M, Nabrdalik K, Gumprecht J, and Stompór T. Inflammation and
538 Oxidative Stress in Diabetic Kidney Disease: The Targets for SGLT2 Inhibitors and GLP-1
539 Receptor Agonists. Int J Mol Sci. 2021;22(19).
540 [43] Yamamoto T, Takabatake Y, Takahashi A, Kimura T, Namba T, Matsuda J, et al. High-Fat
541 Diet-Induced Lysosomal Dysfunction and Impaired Autophagic Flux Contribute to Lipotoxicity
542 in the Kidney. J Am Soc Nephrol. 2017;28(5):1534-51.
543 [44] Nakamura J, Yamamoto T, Takabatake Y, Namba-Hamano T, Minami S, Takahashi A, et al.
544 TFEB-mediated lysosomal exocytosis alleviates high-fat diet-induced lipotoxicity in the kidney.
545 JCI Insight. 2023;8(4).
546 [45] de Vries AP, Ruggenenti P, Ruan XZ, Praga M, Cruzado JM, Bajema IM, et al. Fatty kidney:
547 emerging role of ectopic lipid in obesity-related renal disease. Lancet Diabetes Endocrinol.
548 2014;2(5):417-26.
549 [46] Chen Y, Deb DK, Fu X, Yi B, Liang Y, Du J, et al. ATP-citrate lyase is an epigenetic
550 regulator to promote obesity-related kidney injury. Faseb j. 2019;33(8):9602-15.

Figure 1

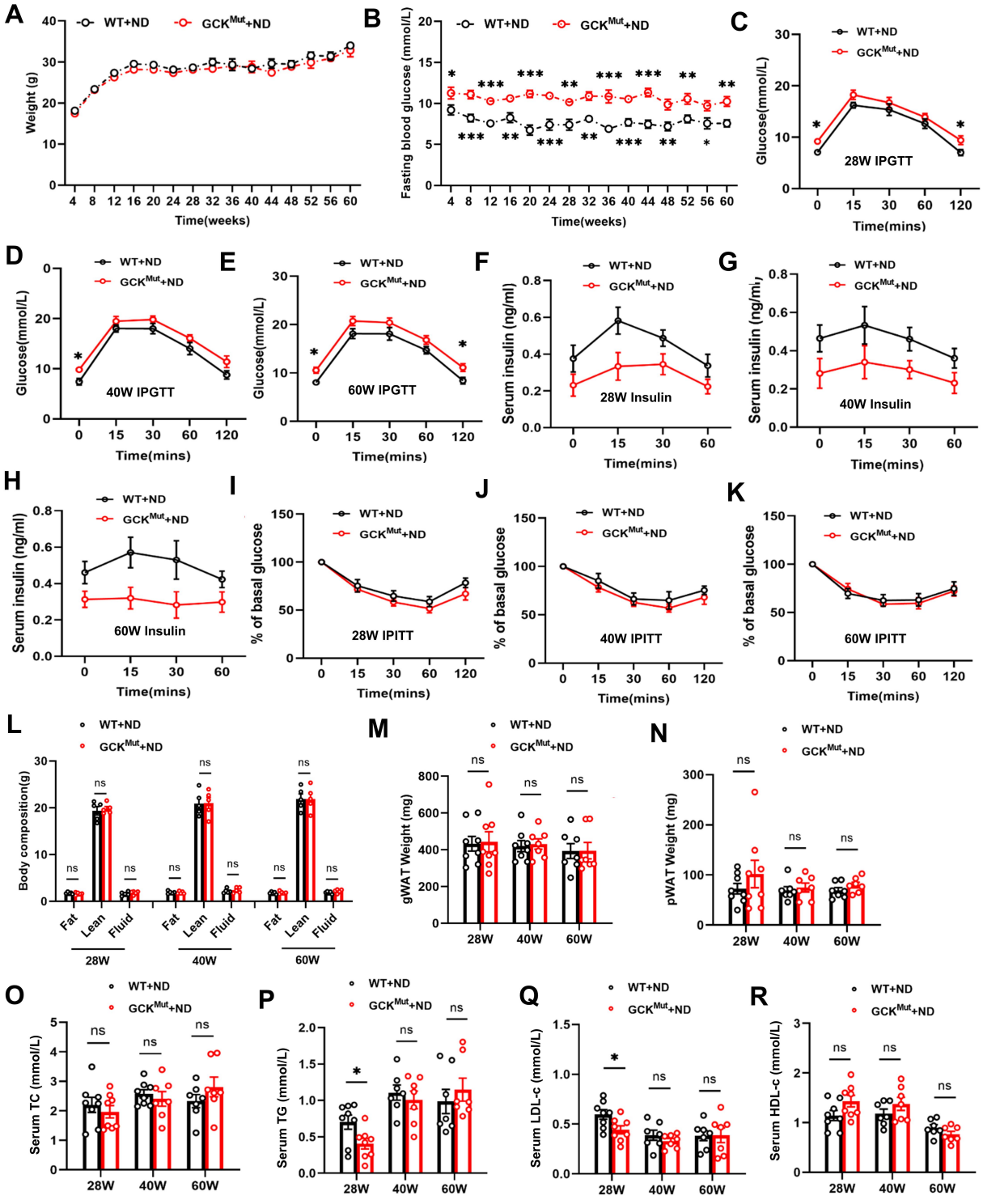

Figure 1. GCK^{Mut} mice had elevated FBG but improved lipids. Body weight (**A**) and fasting blood glucose (**B**) were monitored every 4 weeks (n=7-8 mice/group). (**C-E**) Two groups of

578 mice were intraperitoneally injected with 1 g/kg for IPGTT at 28, 40, or 60 weeks of age
579 (n=5mice/group). (**F-H**) Serum insulin levels were measured by ELISA during IPGTT in both
580 groups of mice (n=5 mice/group). (**I-K**) Two groups of mice were subjected to IPITT
581 (intraperitoneal injection of 0.75 U/kg, n=5mice/group) at 28, 40, or 60 weeks of age. (**L**) Body
582 composition analysis of both groups of mice using a body fat analyzer. (**M-N**) Wet weights of
583 fresh pWAT and gWAT of mice were measured at 28, 40, and 60 weeks of age. Blood samples
584 were used to measure lipid levels including TC (**O**), TG (**P**), LDL-c (**Q**), and HDL-c (**R**), n=5-
585 8mice/group. Values are expressed as mean±SEM. WT+ND vs. GCK^{Mut}+ND: *P<0.05,
586 **P<0.01, ***P<0.001, ns, not significant.
587
588
589
590
591
592
593
594
595
596
597
598
599
600

Figure 2

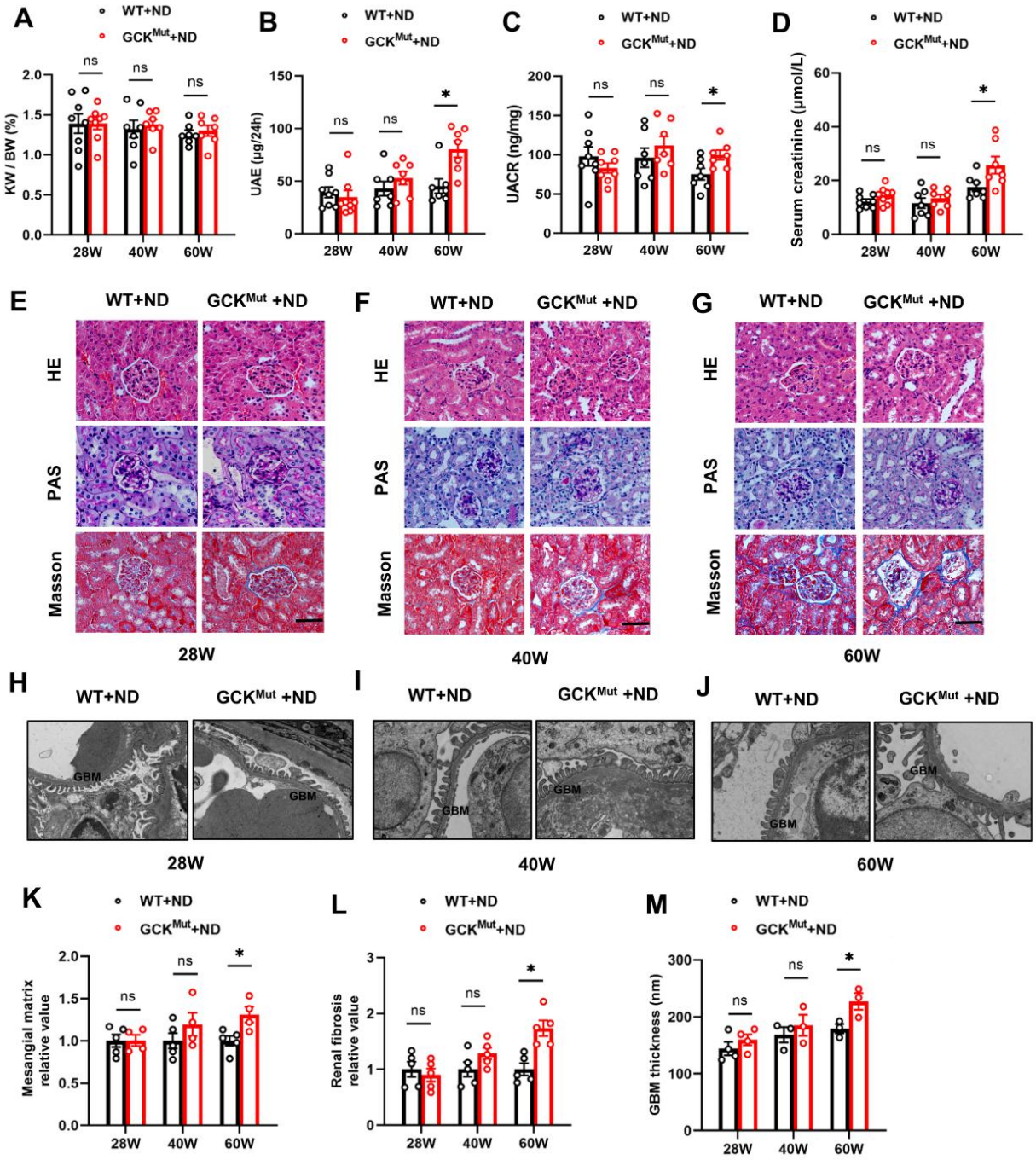

Figure 2. Changes in UAE, serum creatinine and renal histology in GCK^{Mut} mice fed with ND. (**A**) Kidney and body weights were measured at 28, 40, 60-week old, the ratio of kidney and bodyweight (KW/BW) were calculated. 24-hour UAE (**B**), UACR (**C**), and blood creatinine

levels (**D**) were examined in two groups of mice fed with ND at 28, 40, and 60 weeks of age (n=7-8 mice/group). (**E-G**) H&E staining, PAS staining, and Masson staining of kidney sections were performed at 28, 40, and 60 weeks in mice fed with ND (n=5 mice/group). Original magnification = 400. Scale bar = 50μm. (**H-J**) Changes in glomerular structure observed by electron microscopy (n=3 mice/group). Original magnification is x8k. Semi-quantitative analysis of the mesangial matrix (**K**) and the degree of renal fibrosis (**L**). (**M**) Quantification of GBM thickness. Values are expressed as mean±SEM. WT+ND vs. GCK^{Mut}+ND: *$P<0.05$, ns, not significant.

Figure 3

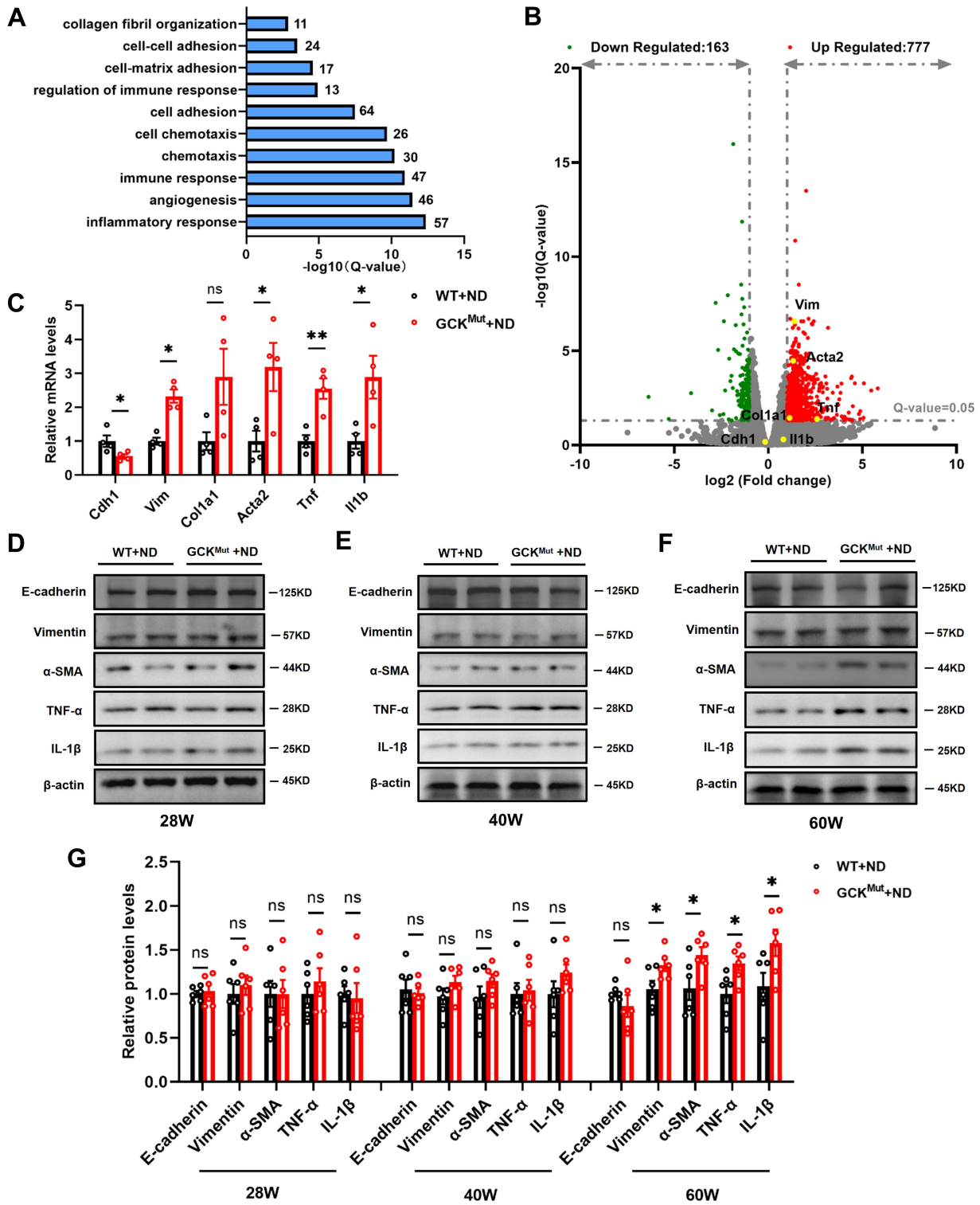
A
collagen fibril organization 11
cell-cell adhesion 24
cell-matrix adhesion 17
regulation of immune response 13
cell adhesion 64
cell chemotaxis 26
chemotaxis 30
immune response 47
angiogenesis 46
inflammatory response 57
-log10（Q-value）
B
Down Regulated:163
Up Regulated:777
-log10(Q-value)
log2 (Fold change)
Vim
Acta2
Tnf
Col1a1
Cdh1
Il1b
Q-value=0.05
C
Relative mRNA levels
WT+ND
GCK^Mut+ND
Cdh1
Vim
Col1a1
Acta2
Tnf
Il1b
D
E
F
WT+ND
GCK^Mut +ND
E-cadherin
Vimentin
α-SMA
TNF-α
IL-1β
β-actin
125KD
57KD
44KD
28KD
25KD
45KD
28W
40W
60W
G
Relative protein levels
WT+ND
GCK^Mut+ND
E-cadherin
Vimentin
α-SMA
TNF-α
IL-1β
28W
40W
60W

631 **Figure 3. Increased renal fibrosis and inflammatory infiltration in 60-week-old GCK^{Mut}**
632 **mice fed with ND.** (**A**) GO analysis of RNA-seq data showed significant changes of pathways in
633 the renal from 60-week-old WT control and GCK^{Mut} mice fed with ND (n=3mice/group). (**B**)
634 Volcano plots depicting transcriptome data, dashed line on the y-axis indicates Q-value=0.05 and
635 fold change on the x-axis is greater than 1. (**C**) The mRNA levels of indicated genes in the
636 kidneys of 60-week-old WT control and GCK^{Mut} mice were determined by qRT-PCR (n=4
637 mice/group). (**D-F**) At 28, 40, and 60 weeks of age, the expression of E-Cadherin, Vimentin, α-
638 SMA, TNF-α, and IL-1β in kidneys of control and GCK^{Mut} mice fed with ND were examined by
639 western blots (n=6 mice/group). (**G**) Quantification of western blots shown in D-F. Values are
640 expressed as mean±SEM. WT+ND vs. GCK^{Mut}+ND: *P<0.05, **P<0.01, ns, not significant.
641
642
643
644
645
646
647
648
649
650
651
652
653

654

Figure 4

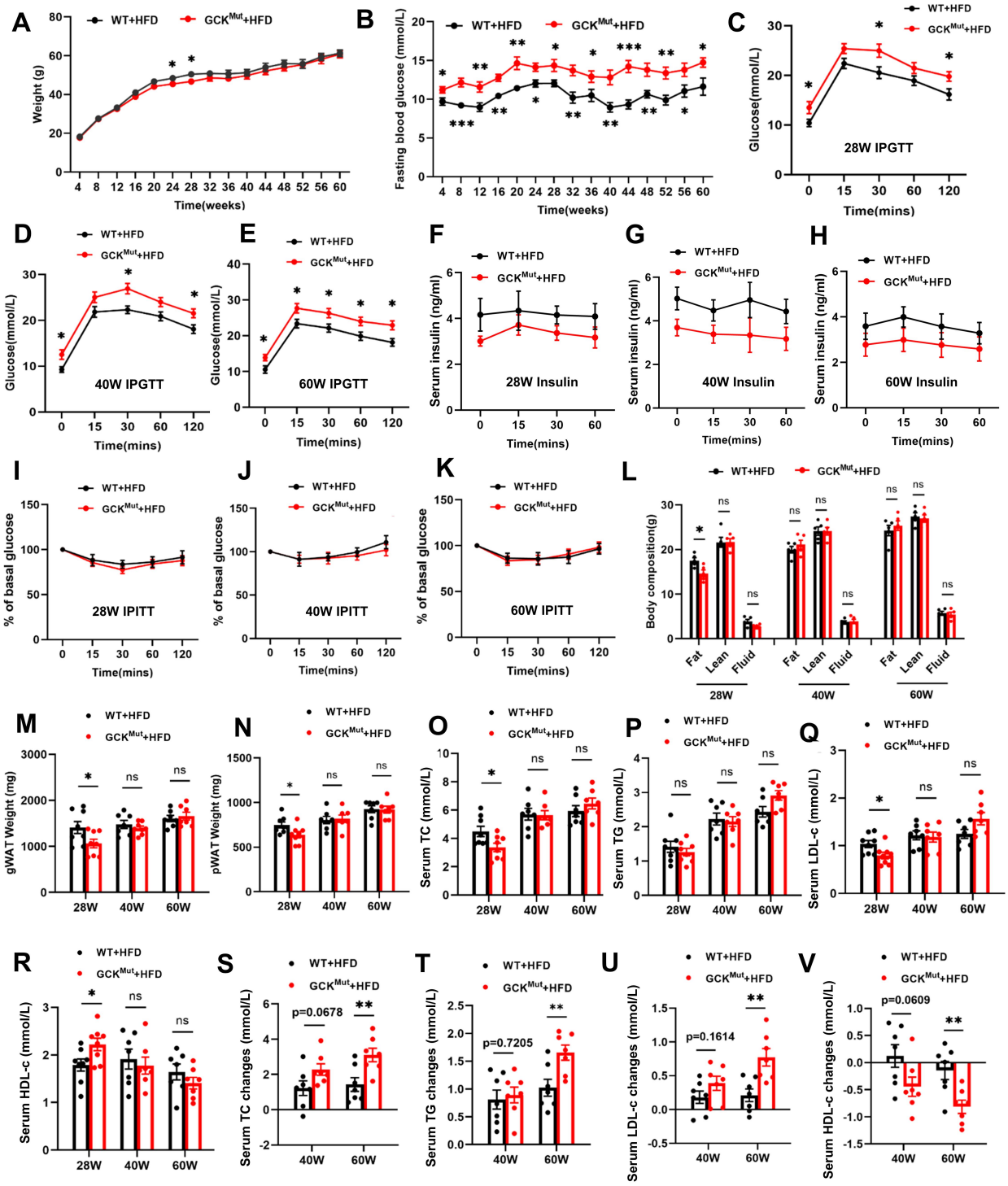

655

656 **Figure 4. Changes in FBG and lipid metabolism in GCK^{Mut} mice fed with HFD.** GCK^{Mut} and
657 control mice were fed with HFD started from 4 weeks of age. The body weight (**A**) and FBG (**B**)
658 have been monthly monitored and recorded till 60 weeks of age. IPGTT were performed in mice
659 fed with HFD at 28 (**C**), 40 (**D**), and 60 (**E**) weeks of age. Serum insulin levels during IPGTT
660 were also measured at 28 (**F**), 40 (**G**), and 60 (**H**) weeks of age. IPITT were performed in mice
661 fed with HFD at 28 (**I**), 40 (**J**), and 60 (**K**) weeks of age (n=5-8 mice/group). (**L**) Body
662 compositions were analyzed in the mice fed with HFD at 28, 40, and 60 weeks of age. (**M-N**)
663 The weight of pWAT and gWAT were measured in the mice above. TC (**O**), TG (**P**), LDL-c (**Q**),
664 HDL-c (**R**) were measured in the mice fed with HFD at 28, 40, and 60 weeks of age. (**S-V**)
665 Changes of TC, TG, LDL-c, HDL-c in mice aged 40 weeks and 60 weeks compared with those
666 aged 28 weeks. n=5-8 mice/group. Values were expressed as mean±SEM. WT+HFD vs.
667 GCK^{Mut}+HFD: *P<0.05, **P<0.01, ***P<0.001, ns, not significant.

668
669
670
671
672
673
674
675
676
677
678
679
680
681

682

Figure 5

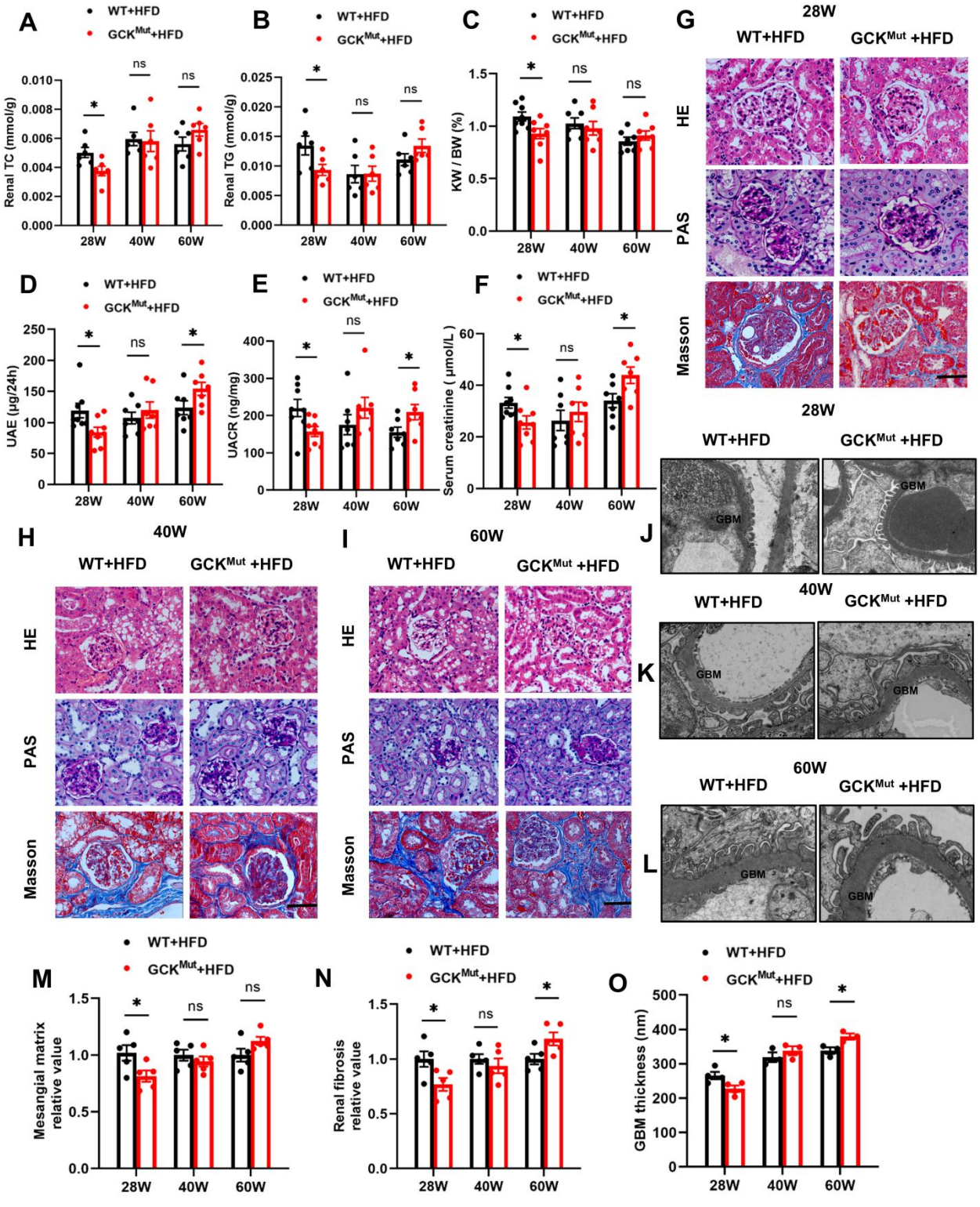

683

684 **Figure 5. GCK^{Mut} attenuated HFD associated renal injury at 28 weeks of age, but**
685 **aggravated renal injury at 60 weeks of age.** Renal TC (**A**), Renal TG (**B**), KW/BW (**C**), 24-
686 hour UAE (**D**), UACR (**E**), and serum creatinine levels (**F**) were examined at 28, 40, and 60
687 weeks of age in both groups of mice (n=7-8 mice/group). (**G-I**) H&E staining, PAS staining, and
688 Masson staining of renal sections at 28, 40, and 60 weeks in both groups of mice (n=5
689 mice/group). Original magnification = 400. Scale bar = 50μm. (**J-L**) Electron microscopic
690 observation of changes in glomerular structure in two groups of mice (n=3 mice/group). Original
691 magnification is x8k. Semi-quantitative analysis of the mesangial matrix (**M**) and the degree of
692 renal fibrosis (**N**). Quantification of GBM thickness (**O**). Values are expressed as mean±SEM.
693 WT+HFD vs. GCK^{Mut}+HFD: *P<0.05, ns, not significant.
694
695
696
697
698
699
700
701
702
703
704
705
706

Figure 6

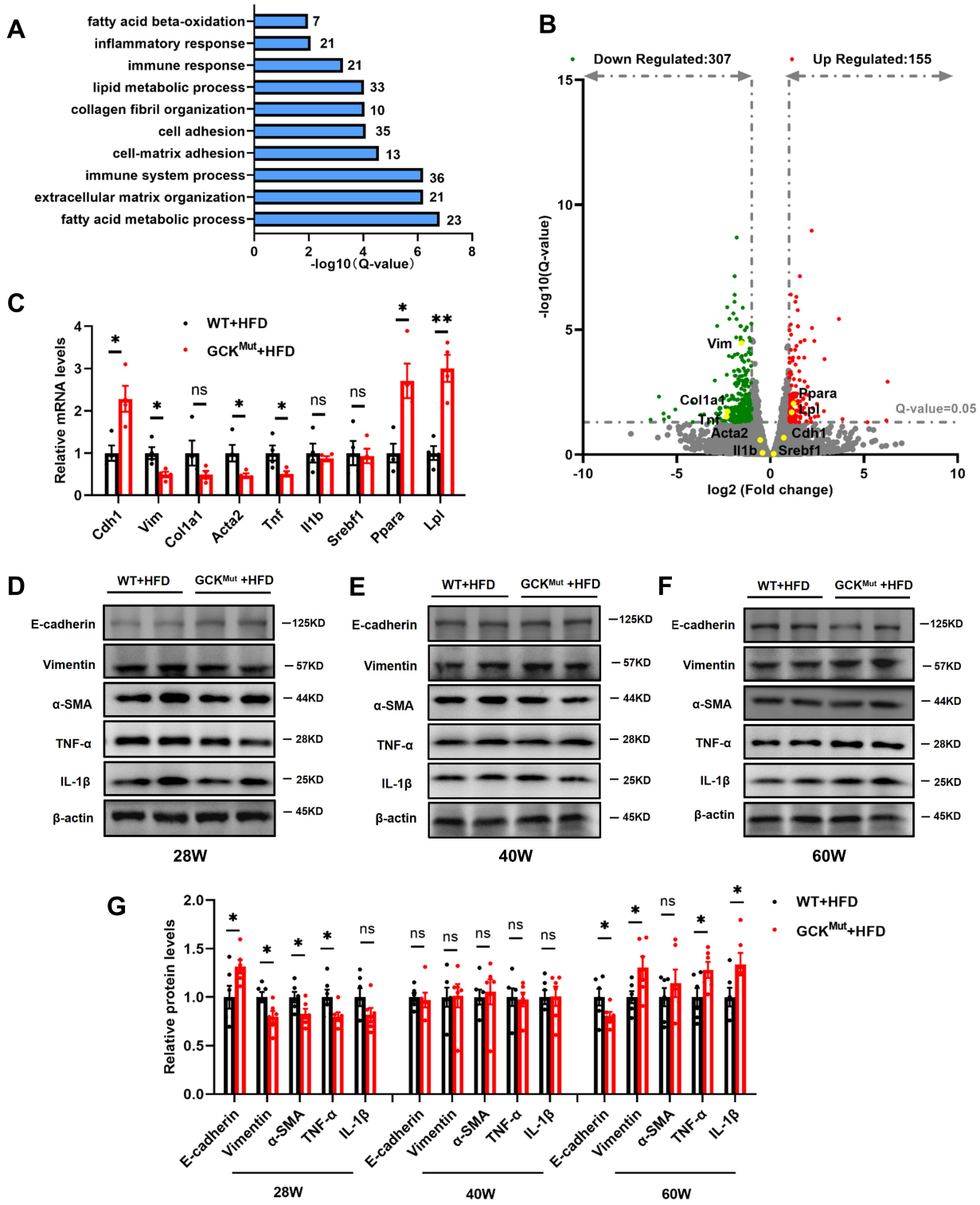
A
fatty acid beta-oxidation 7
inflammatory response 21
immune response 21
lipid metabolic process 33
collagen fibril organization 10
cell adhesion 35
cell-matrix adhesion 13
immune system process 36
extracellular matrix organization 21
fatty acid metabolic process 23
-log10（Q-value）
B
Down Regulated:307
Up Regulated:155
-log10(Q-value)
log2 (Fold change)
Q-value=0.05
Vim
Col1a1
Tnf
Acta2
Il1b
Ppara
Lpl
Cdh1
Srebf1
C
WT+HFD
GCKMut+HFD
Relative mRNA levels
Cdh1
Vim
Col1a1
Acta2
Tnf
Il1b
Srebf1
Ppara
Lpl
D
E
F
WT+HFD
GCKMut +HFD
E-cadherin
Vimentin
α-SMA
TNF-α
IL-1β
β-actin
125KD
57KD
44KD
28KD
25KD
45KD
28W
40W
60W
G
Relative protein levels
WT+HFD
GCKMut+HFD
E-cadherin
Vimentin
α-SMA
TNF-α
IL-1β
28W
40W
60W

709 **Figure 6. Renal fibrosis and inflammatory were attenuated in HFD GCK^{Mut} mice at 28**
710 **weeks of age and aggravated at 60 weeks of age**. (**A**) The GO analysis of data obtained by
711 RNA-Seq showed significantly different gene enrichment (n=3 mice/group). (**B**) Volcano plots
712 depicting transcriptomics data, dashed line on the y-axis indicates Q-value=0.05 and fold change
713 on the x-axis is greater than 1. (**C**) The mRNA levels of the mentioned factors in the kidneys of
714 28-week-old HFD WT control and GCK^{Mut} mice were determined by qRT-PCR (n=4
715 mice/group). (**D-F**) Renal E-Cadherin, Vimentin, α-SMA, TNF-α, and IL-1β protein levels were
716 detected by Western blot analysis at 28, 40, and 60 weeks of age (n=6 mice/group). (**G**) Results
717 of quantitative immunoblot analysis for each group. Values are expressed as mean±SEM.
718 WT+HFD vs. GCK^{Mut}+HFD: *P<0.05, **P<0.01, ***P<0.001, ns, not significant.
719
720
721
722
723
724
725
726
727
728
729
730
731

Supplemental Figure 1

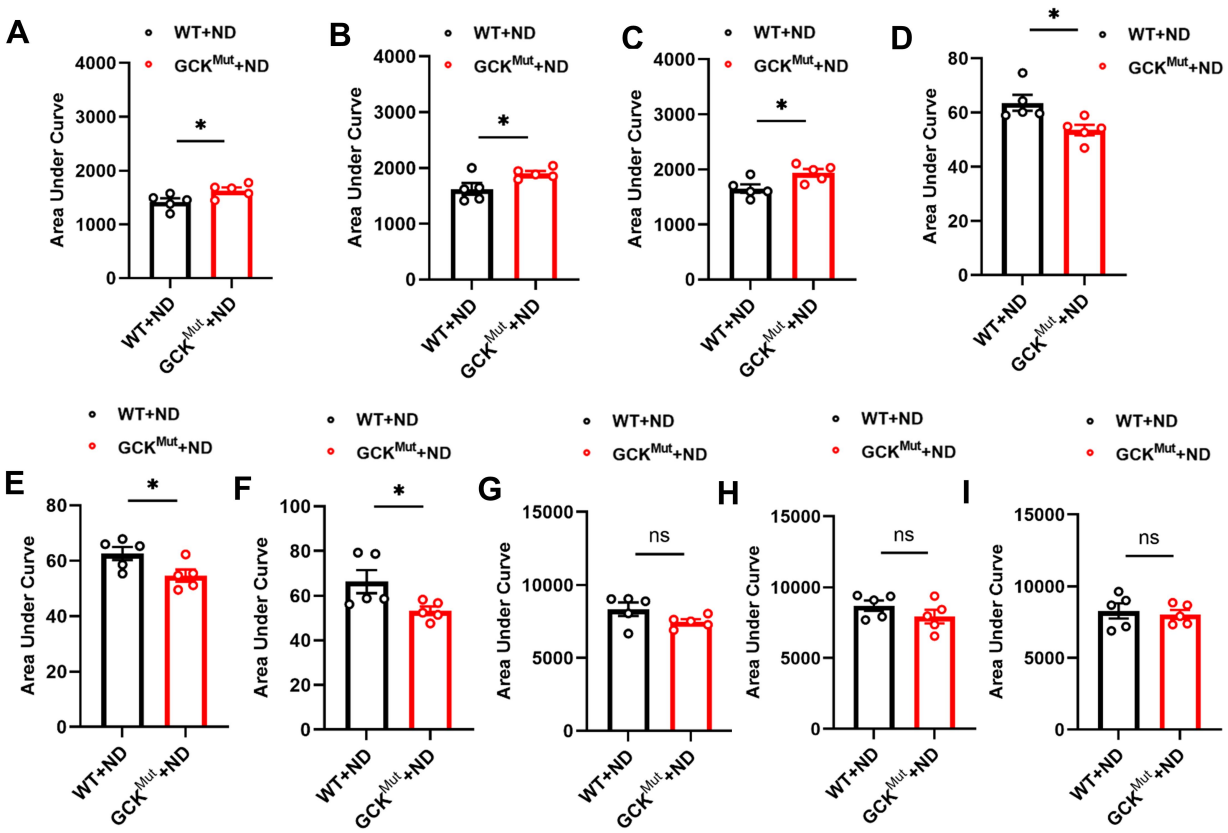

Supplemental Figure 1. The area under the curve (AUC) of IPGTT, serum insulin and IPITT in two groups of mice on ND. (**A-C**) The AUCs of blood glucose levels were calculated according to Fig.1C-E. (**D-F**) The AUCs of serum insulin levels were calculated from Fig. 1F-H. (**G-I**) The AUCs of blood glucose during IPITT were calculated from Fig.1I-K. n=5mice/group. Values are expressed as mean±SEM. WT+ND vs. GCK^{Mut}+ND: *P<0.05, ns, not significant.

744 **Supplemental Figure 2**

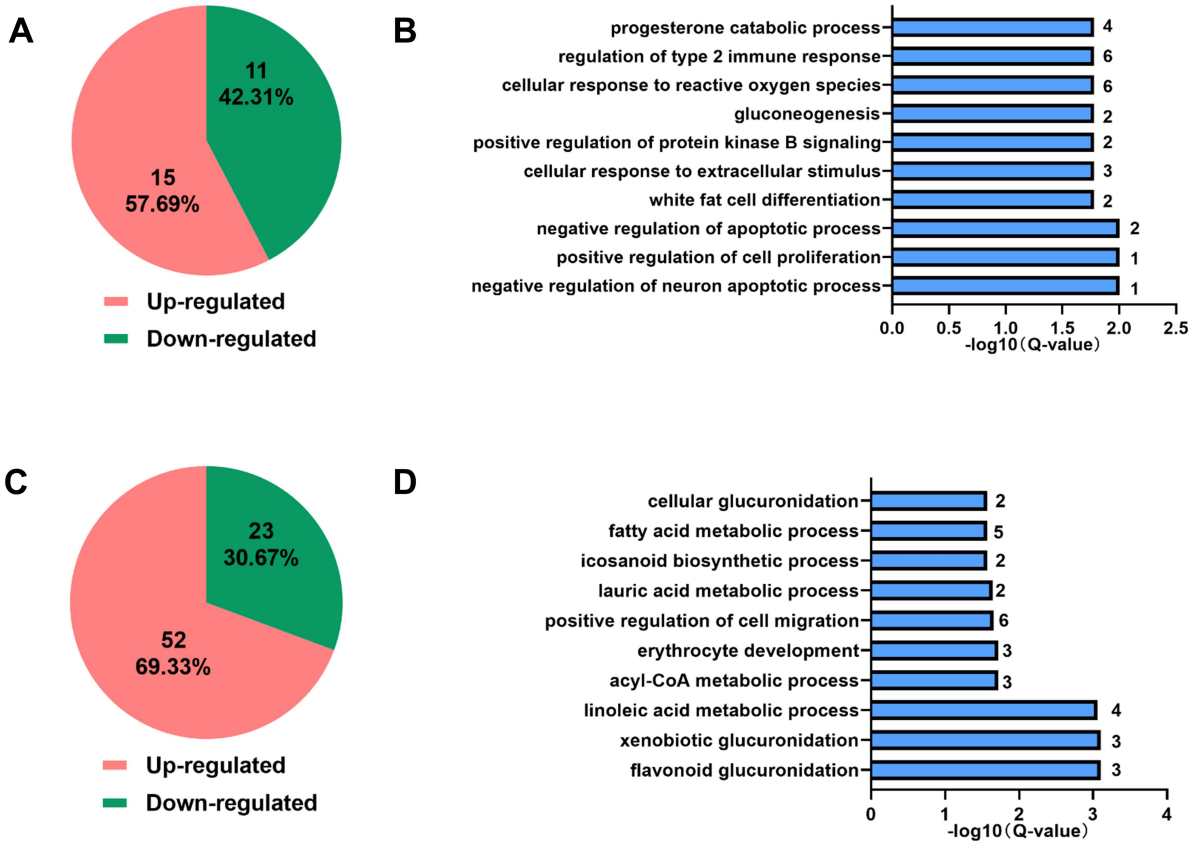

745

746 **Supplemental Figure 2. The kidney transcriptome analysis at 28 and 40 weeks in two**
747 **groups of mice on ND.** (**A-B**) The number of significantly different genes up- and down-
748 regulated and GO analysis in two groups of mice on regular diet at 28 weeks of age. (**C-D**) The
749 number of significantly different genes up- and down-regulated and GO analysis in two groups
750 of mice on ND at 40 weeks of age. n=3 mice/group.

751

752

753

754

755

Supplemental Figure 3

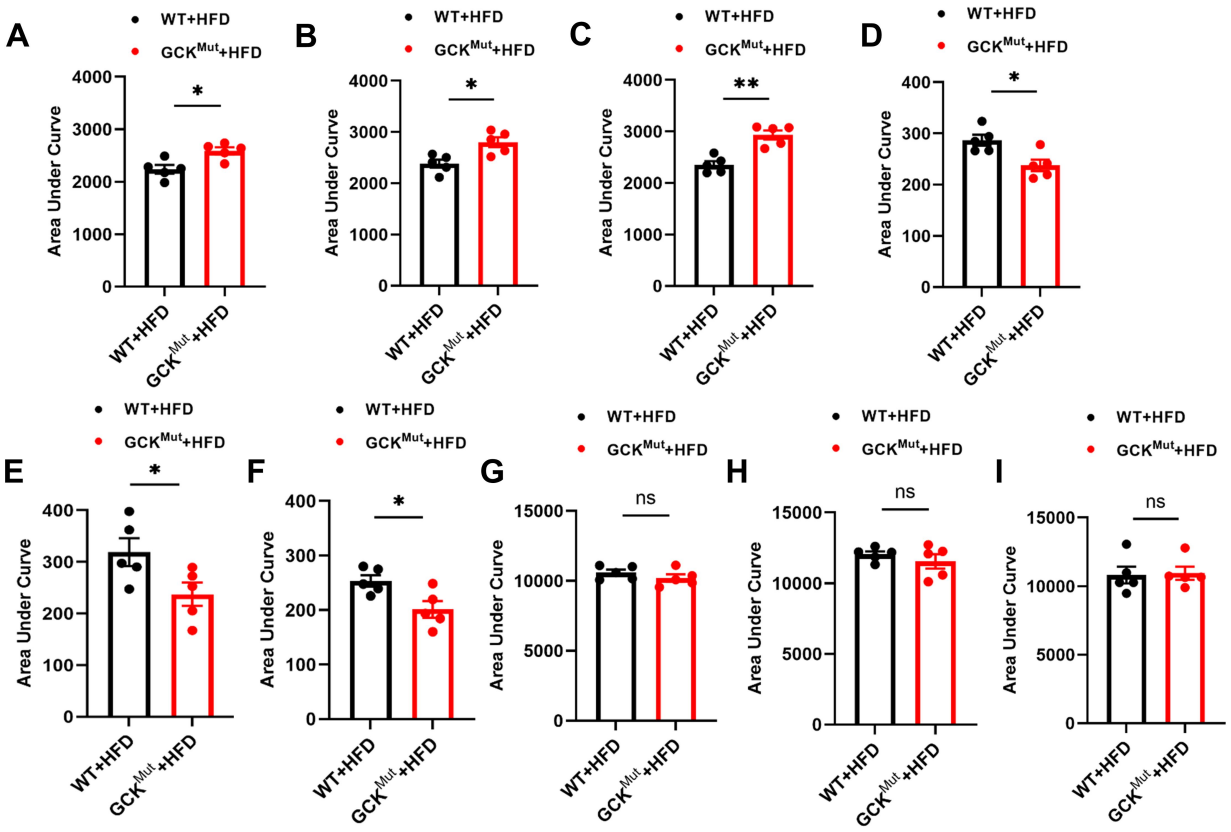

Supplemental Figure 3. The area under the curve (AUC) of IPGTT, serum insulin, and IPITT in two groups of mice fed with HFD. (**A-C**) The AUC of IPGTT was calculated according to Figure.5C-E. (**D-F**) The AUC for serum insulin levels was calculated from Figure.5F-H. (**G-I**) The AUC values for IPITT were calculated from Figure.5I-K. n=5 mice/group. Values are expressed as mean±SEM. WT+HFD vs. GCK^{Mut}+HFD: *P<0.05, ns, not significant.

769 **Supplemental Figure 4**

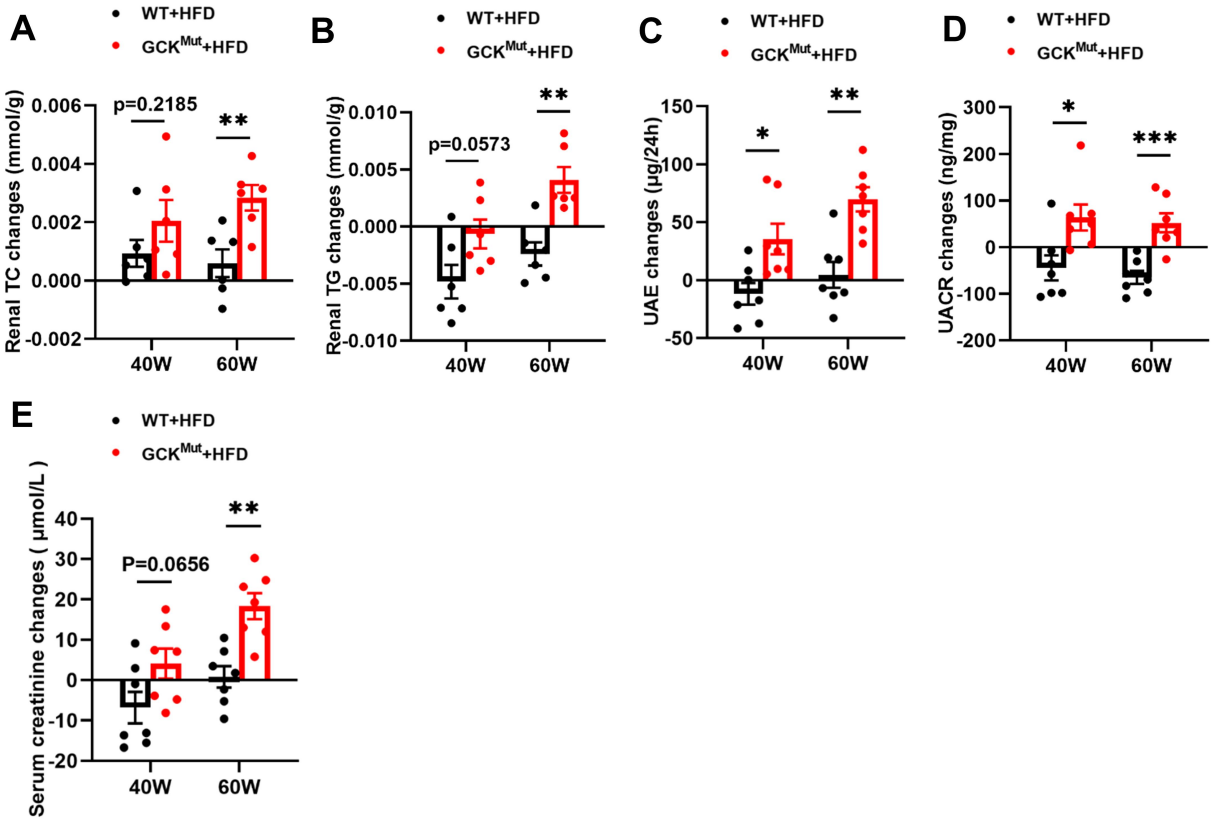

770

771 **Supplemental Figure 4. Changes of Renal TC, Renal TG, 24-hour UAE, UACR, and serum**
772 **creatinine in mice aged 40 weeks and 60 weeks compared with those aged 28 weeks fed with**
773 **HFD.** Changes of Renal TC (**A**), Renal TG (**B**), 24-hour UAE (**C**), UACR (**D**), and serum
774 creatinine (**E**) in mice aged 40 weeks and 60 weeks compared with those aged 28 weeks. Values
775 were expressed as mean±SEM. WT+HFD vs. GCK^{Mut}+HFD: *P<0.05, **P<0.01, ***P<0.001,
776 ns, not significant.

777

778

779

780

781 **Supplemental Figure 5**

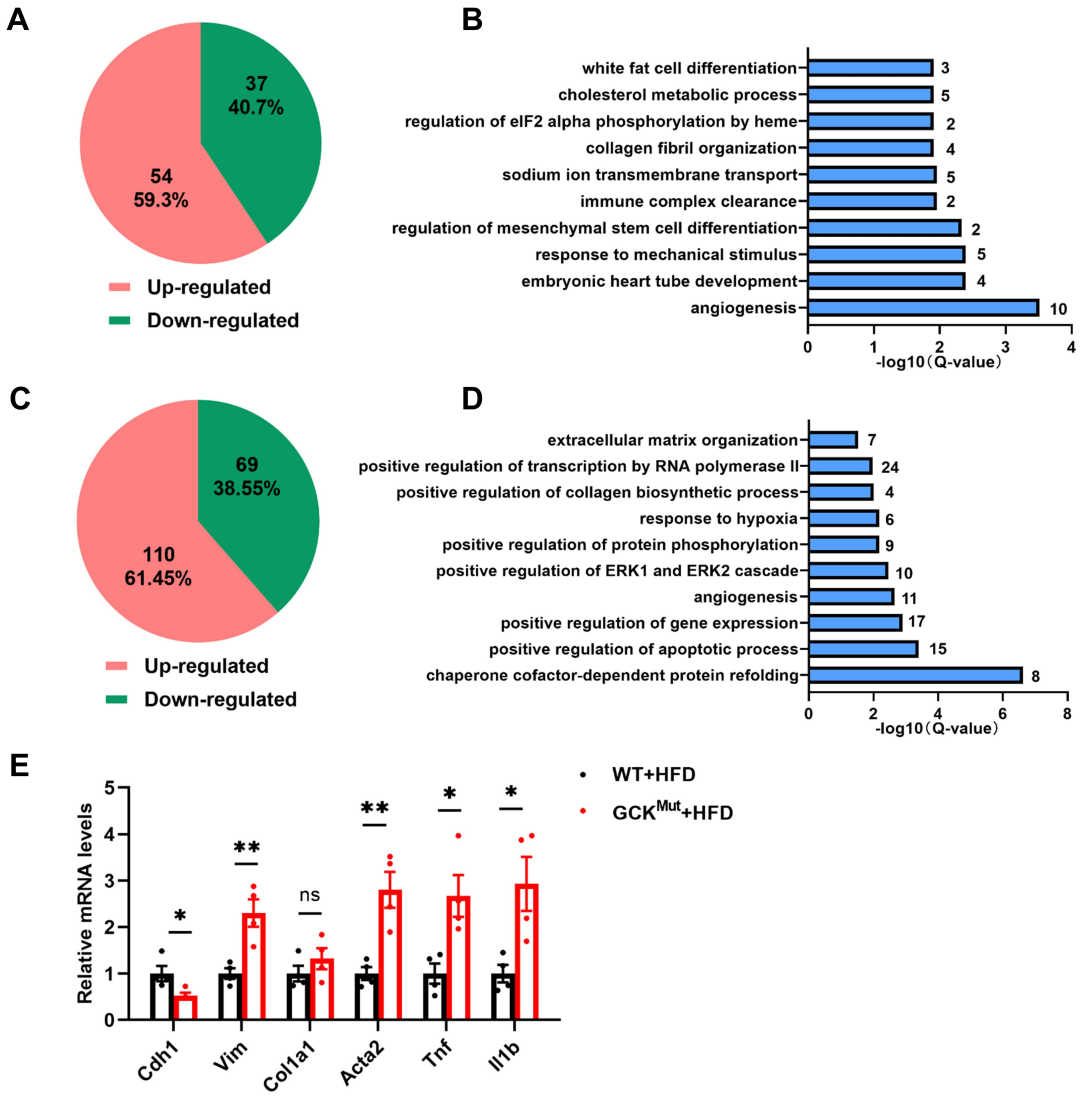

782

783 **Supplemental Figure 5. The kidney transcriptome analysis at 40 and 60 weeks in two**
784 **groups of mice on HFD.** (**A-B**) The number of significantly different genes up- and down-
785 regulated and GO analysis in two groups of mice on HFD at 40 weeks of age. (**C-D**) The number
786 of significantly different genes up- and down-regulated and GO analysis in two groups of mice
787 on HFD at 60 weeks of age. (**E**) The mRNA levels of relevant fibrosis and inflammatory factors
788 in the kidneys of two groups of mice on HFD at 60 weeks of age.

789

790

Supplemental Table 1. Primer sequences (m-Mus musculus) for qRT-PCR (5'-3')

Gene	Forward	Reverse
mCdh1	CAGGTCTCCTCATGGCTTTGC	CTTCCGAAAAGAAGGCTGTCC
mVim	CGGCTGCGAGAGAAATTGC	CCACTTTCCGTTCAAGGTCAAG
mCol1a1	ATGTTCAGCTTTGTGGACCTC	CAGAAAGCACAGCACTCGC
mActa2	GTCCCAGACATCAGGGAGTAA	TCGGATACTTCAGCGTCAGGA
mTNF-α	GCGACGTGGAACTGGCAGAAGAGG	GTACTTGGGCAGATTGACCTCAGC
mIL-1β	CACTACAGGCTCCGAGATGAACAAC	TGTCGTTGCTTGGTTCTCCTTGTAC
mSrebf1	GGAGCCATGGATTGCACATT	GGCCCGGGAAGTCACTGT
mPpara	AGAGCCCCATCTGTCCTCTC	ACTGGTAGTCTGCAAAACCAAA
mLpl	GGGAGTTTGGCTCCAGAGTTT	TGTGTCTTCAGGGGTCCTTAG
mGAPDH	ACCCACTCCTCCACCTTTGAC	TGTTGCTGTAGCCAAATTCGTT

791

792